Effects of polyolefin elastomer on physico-mechanical and thermal properties of HDPE/CaCO₃/LDPE-g-MA/POE composites

Youngjun Ahn*, Ji Whan Ahn**, and Choon Han*,†

*Department of Chemical Engineering, Kwangwoon University, 20 Gwangun-ro, Nowon-gu, Seoul 01897, Korea
**Mineral Resources Research Division, Korea Institute of Geoscience and Mineral Resources,
124 Gwahak-ro, Yuseong-gu, Daejeon 34132, Korea

Abstract−The HDPE/CaCO₃/LDPE-g-MA/POE composite was prepared by blending high density polyethylene (HDPE) filled calcium carbonate (CaCO₃), with maleic anhydride grafted low density polyethylene (LDPE-g-MA) as a compatibilizer, and a polyolefin elastomer (POE). The composites exhibited improved tensile strength than composites without POE. The addition of POE led to a decrease in the d-spacing of CaCO₃, indicating that core-shell structure was formed between POE and CaCO₃. Because of good dispersion of CaCO₃, this improved thermal stability and decreased crystallinity (X_c) and conformational change (ΔS_c). The composites contributed to improved mechanical property and good dispersion of CaCO₃, and efficient activation energy by accelerating the crystallization rate.

Keywords: Polymer Composite, Polyethylene, Calcium Carbonate, Polyolefin Elastomer

INTRODUCTION

A thermoplastic elastomer (TPE) has the properties of a thermoplastic material and rubber. TPE is one of the most important materials currently being used in various fields, including automobile parts, electric wires, fibers, adhesives, and pavement. Furthermore, TPE contains useful properties of a crystal or a glassy hard block as a reversible physical cross-linker [1,2].

Generally, TPE consists of a hard phase and a soft phase. The reaction of chains is limited in the hard phase because the reaction temperature of the hard phase is higher than the glass transition temperature and the melting temperature, whereas the soft phase comprises components having a reaction temperature lower than the glass transition temperature and the melting temperature. The ratio of the quantity of one phase to that of another phase determines whether a TPE has a dispersed or continuous phase, which in turn determines the physical properties of the TPE [3]. TPEs have excellent physical properties, including the outstanding processing capacity of thermoplastic materials and the elasticity of rubber. There are different types of TPE, including olefin TPE and styrene TPE [1,3]. In particular, olefin TPE, also called polyolefin elastomer (POE), is a novel type of copolymer that was developed following advances in the development of the metallocene polymerization catalyst. Compared with olefin polymers that are polymerized using a conventional Ziegler-Natta catalyst, the POE has better mechanical properties, including better tensile and impact strengths. POE has replaced many conventional polymers, because POE has high compatibility with various polyolefin materials, good recyclability, excellent impact strength, weather resistance, and a low

price. Ethylene-based POEs include an ethylene monomer and comonomers such as 1-butene, 1-hexene, and 1-octene. Propylene-based POEs use 1-propylene as a comonomer [1].

To improve the polymer/TPE blending properties, composites have been studied by adding SiO₂, organoclay, and calcium carbonate (CaCO₃). The tensile and impact strengths may be effectively increased by using a small quantity of filler in these composites. The addition of nanofillers (e.g. clays) results in an improvement in the physicochemical, mechanical, thermal and barrier properties of composite materials [4-6,10]. In addition, polypropylene (PP)/filler/ rubber composites have been applied in various fields including automobile, electric wire, electronic devices, and packaging materials [7-15]. The addition of hydrophilic nano-SiO₂ particles to PP/ ethylene propylene rubber (EPDM), and maleic anhydride grafted PP (PP-g-MA)/EPDM, improved the toughness and stiffness of these composites [7]. The addition of organoclay to polypropylene-ethylene-propylene (PP-EP)/ethylene vinyl acetate (EVA) increased the fire retardancy of the composite [8]. In addition, the organoclay added to the PP/POE/PP-g-MA was dispersed as nano-particles and increased the melting temperature, as the organoclay played the role of a nucleating agent [9]. An intercalation type composite was prepared by adding organoclay to PP/EPDM, and the addition of the organoclay increased the tensile strength and elongation at break [10]. Using a continuous twin extruder to add organoclay to PP/styrene-6-(ethylene-co-butylenes)-6-styrene triblock copolymer (SEBS), improved different parameters. For instance, the tensile strength, modulus, flexibility, and impact strength were found at a specific amount of added organoclay [11]. Ma et al. [12] added nano-CaCO₃ particles to PP/POE and found an improvement in the impact resistance of the composites. However, many studies have focused on improving the mechanical properties of the PP matrix based materials using various inorganic substances, including CaCO₃ particles for surface treatment, and by adding nano-

†To whom correspondence should be addressed.
E-mail: chan@kw.ac.kr

sized inorganic substances.

Our purpose was to investigate the novel behavior of the composites prepared by two types of POE, to high density polyethylene (HDPE)/CaCO$_3$ composite using maleic anhydride grafted low density polyethylene (LDPE-g-MA) as a compatibilizer. An experiment was conducted to investigate the tensile strength, thermal properties and other features of a crystal structure. In addition, samples having high tensile strengths were selected to examine their non-isothermal crystallization behaviors and activation energies (E$_a$).

EXPERIMENTAL

1. Materials

The materials used for preparing the HDPE/CaCO$_3$/LDPE-g-MA/POE composite included HDPE (LG Chemical Co. Korea) and CaCO$_3$ (Duksan Co. Korea). LDPE-g-MA [13] having the highest grafting degree of 4.88% was prepared and added. LC565 (LC POE), an ethylene-based POE, was provided by LG Chemical Co., Korea, and Vistamaxx 6102 (VM POE), a propylene-based POE, was obtained from ExxonMobile.

2. Preparation of the HDPE/CaCO$_3$/LDPE-g-MA/POE Composites

Prior to use, CaCO$_3$ was dried for eight hours in a vacuum oven at 80 °C to remove moisture. Different types of POE were added to the HDPE/CaCO$_3$/LDPE-g-MA composites, respectively, which were then melt mixed (Table 1) in a Haake mixer (Rheomix 600, Germany) at 50 rpm for five minutes at 140 °C. Samples were prepared by compression molding performed for two minutes at 130 °C using a hot press (Carver, USA). The samples were then cold pressed between two plates for three minutes at room temperature.

3. Characterization of the HDPE/CaCO$_3$/LDPE-g-MA/POE Composites

3-1. Tensile Strength

The tensile strength of the composites was measured with a universal testing machine (UTM, Tiniusolsen, USA) at room tempera-

Table 1. Description of the HDPE/CaCO$_3$/LDPE-g-MA/POE composites[a]

Sample name	HDPE	CaCO$_3$	LDPE-g-MA	VM POE	LC POE
HCLV1	3	7		3	-
HCLV2	3	7		7	-
HCLV3	3	7		10	-
HCLV4	7	3		3	-
HCLV5	7	3		7	-
HCLV6	7	3		10	-
HCLL1	3	7	10	-	3
HCLL2	3	7		-	7
HCLL3	3	7		-	10
HCLL4	7	3		-	3
HCLL5	7	3		-	7
HCLL6	7	3		-	10

[a]All numerical values show the weight ratio (%) to the composites

ture in accordance with ASTM D638. All measurements were taken at a head speed of 10 mm/min, and average values were obtained from five repeated tests.

3-2. X-ray Diffraction (XRD)

The crystal structure of the HDPE/CaCO$_3$/LDPE-g-MA/POE composites was determined by X-ray diffraction (XRD, Rigaku, Japan) with Cu Kα radiation (λ=0.154 nm) at room temperature within a 2θ range from 10 to 50 degrees. To demonstrate these findings, the d-spacing of HDPE/CaCO$_3$/LDPE-g-MA/POE composites was calculated by using Bragg's law:

$$\lambda = 2d \sin\theta \tag{1}$$

where λ is the wavelength of the incident radiation, d is the interplanar spacing (nm), and θ is the scattering angle.

3-3. Thermogravimetric Analysis (TGA)

Thermogravimetric analysis (TGA, TGA Q500, USA) was performed to assess the thermal stability of all composites. The samples were heated at 5 °C/min from 25 °C to 900 °C under a nitrogen atmosphere.

3-4. Differential Scanning Calorimeter (DSC)

To examine non-crystallization behavior and kinetic, differential scanning calorimetry (DSC, DSC Q1000, USA) was carried out at a cooling rate of 5 °C/min from 200 °C to room temperature under a nitrogen atmosphere. The crystallinity (X$_c$) of the composites was determined by the following:

$$X_c(\%) = \frac{\Delta H_C}{(1-\omega) \times \Delta H^*} \times 100 \tag{2}$$

where X$_c$ is the crystallinity (%), ΔH_c is the measured melting enthalpy (J/g), ΔH^* is the melting enthalpy of HDPE (293 J/g) [16], and ω is the weight fraction of HDPE in the composites. In addition, the conformational change during the crystallization was obtained by using the entropy of crystallization (ΔS_c) as calculated by the following equation [17]:

$$\Delta S_c = \frac{\Delta H_c}{T_c} \tag{3}$$

where ΔH_c is the enthalpy of crystallization, and T$_c$ is the crystallization temperature. Furthermore, relative crystallinity (X$_T$) calculated by using following was compared to HDPE and the composites:

$$X_T = \frac{\int_{T_o}^{T} (dH_c/dT)dT}{\int_{T_o}^{T_f} (dH_c/dT)dT} \tag{4}$$

where T$_o$ and T$_f$ are the onset and finishing temperature of crystallization, respectively, and dH$_c$/dT is the heat flow rate. Crystallization time (t), in relation to temperature was calculated as follows:

$$t = \frac{(T_o - T_c)}{\alpha} \tag{5}$$

where T$_o$ and T$_c$ are the onset and crystallization temperature, respectively, and α is the cooling rate.

The Avrami model is the most frequently used in the study of the crystallization dynamics of polymer and composites [18] to analyze dynamic isothermal crystallization as in the following equation:

$$\ln[-\ln(1-X_t)] = Z_t + n\ln t \qquad (6)$$

where X_t denotes the relative crystallinity, n is the Avrami exponent, and Z_t is the time-dependent crystallization rate constant. The most frequently used method is the model derived from the Avrami model by Jeziorny [19], where the crystallization rate constant is determined by using the cooling rate, as shown in the following:

$$\ln Z_c = \frac{\ln Z_t}{\alpha} \qquad (7)$$

Furthermore, the activation energy (E_a) of HDPE and the composites was calculated by using the DSC data by the Kissinger method [20]:

$$\ln \frac{\alpha}{T_c^2} = -\frac{E_a}{R} \frac{1}{T_c} \qquad (8)$$

where α is the cooling rate, T_c is the crystallization temperature and R is the gas constant.

RESULTS AND DISCUSSION

1. Tensile Strength Analysis

The mechanical properties of a composite may be changed by various conditions, including the interaction between the components. Compatibilities may be increased or decreased depending on the conditions. The effect of composite compatibility on physical properties was investigated by varying the weight ratio while keeping a fixed ratio of LDPE-g-MA. The tensile strengths of the HDPE/CaCO₃/LDPE-g-MA/POE composites are shown in Fig. 1. The tensile strength of all the composites prepared in the present study was higher than that of the composite without POE [13]. In addition, the tensile strength of all the composites was decreased as the ratio of the two types of POE was increased, and higher tensile strength was obtained from a sample with a higher ratio of HDPE.

The tensile strength was higher in the composites to which LC

POE was added than in the composites to VM POE containing composites. The result indicates that the interfacial adhesion is stronger between the HDPE matrix and the ethylene-based LC POE. Similarly, Liang et al. [21] reported that the tensile strength and elongation at break of PP/POE/nano-CaCO₃ increased with increasing ratios of POE, suggesting that conformational change inside the composite may be correlated with the mechanical properties. Xie et al. [22] added amino acid-treated CaCO₃ particles and untreated CaCO₃ particles to HDPE and maleated poly(ethylene-octene) (POE-g), and investigated the mechanical properties of the materials. The surface-treated CaCO₃ particles showed increased affinity to the matrix and higher tensile strength, but the tensile strength was decreased as the ratio of POE-g was increased. Sampath et al. [23] added a titanate coupling agent to CaCO₃-filled natural rubber, LDPE and examined the mechanical properties. The tensile strength decreased as the ratio of added LDPE increased over a specific level, indicating that a high ratio of LDPE decreased the activity of the titanate coupling agent, preventing good dispersion of the CaCO₃ particles, and thus decreasing the tensile strength.

In addition, since a composite is affected by the melt flow index (MFI) of the POE, entanglement may be caused, depending on the molecular weight, the molecular weight distribution, and the chain length, and the MFI of PE has been reported to be rapidly changed due to the chain structure [24]. The chain entanglement of HDPE may reduce the fluidity of HDPE because of steric hindrance by the branched molecular structure of POE [25]. For the above reasons, the tensile strength of HDPE/CaCO₃/LDPE-g-MA/POE composites decreased with increasing the ratio of two POEs, respectively. The tensile strength of the composites by adding LC POE was found to be higher due to the longer branch structure of the LC POE in comparison with the propylene-based VM POE. The above results indicated that when steric hindrance occurs, POE of the matrix as a similar structure or longer branch structure plays an important role in enhanced interaction with matrix and improved tensile strength.

2. XRD Analysis

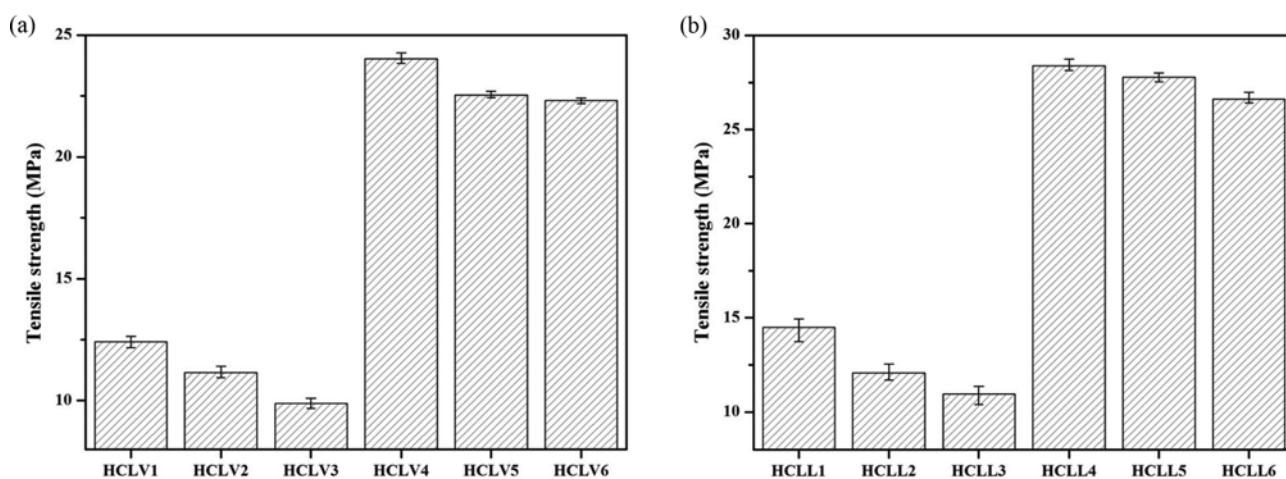Two types of composites with POE can generally be prepared:

Fig. 1. Tensile strength of composites: (a) HDPE/CaCO₃/LDPE-g-MA/VM POE composites, (b) HDPE/CaCO₃/LDPE-g-MA/LC POE composites.
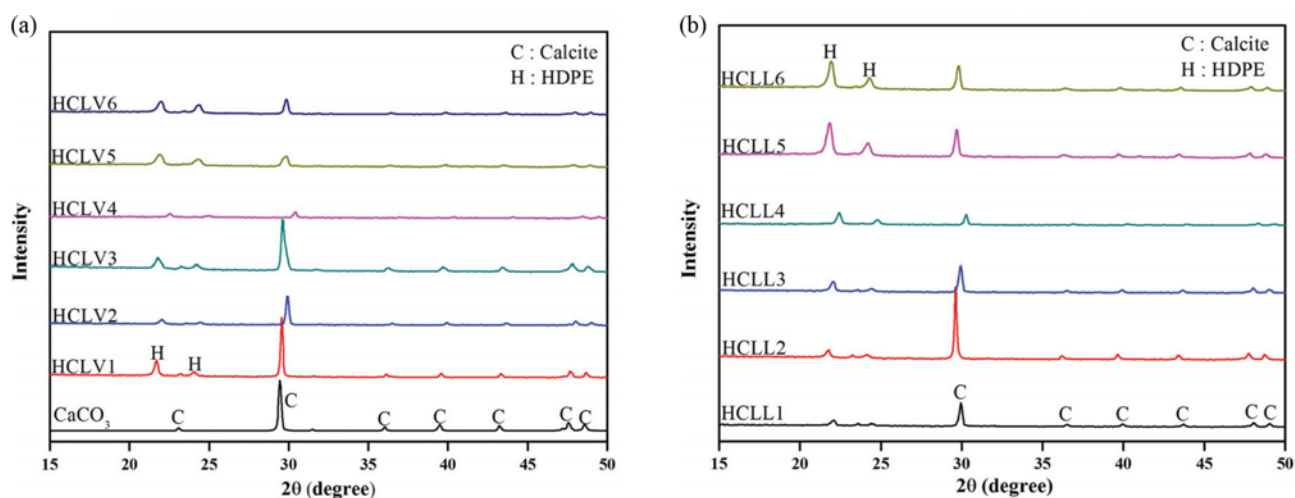
Fig. 2. XRD peaks of composites: (a) HDPE/CaCO₃/LDPE-g-MA/VM POE composites, (b) HDPE/CaCO₃/LDPE-g-MA/LC POE composites.

(1) the POE and inorganic substance are, respectively, dispersed in the matrix to form independently dispersed phase, and (2) the POE encapsulates the inorganic substance to form a core-shell structure where POE serves as a shell and the inorganic substance as a core.

Table 2. XRD peak conditions of HDPE/CaCO₃/LDPE-g-MA/POE composites

Sample name	Angle (2 theta)	d-Spacing (nm)	hkl
HDPE	22.55	0.394	(110)
CaCO₃	29.45	0.303	(104)
HCLV1	21.7	0.409	(110)
	29.55	0.302	(104)
HCLV2	22.05	0.403	(110)
	29.9	0.299	(104)
HCLV3	21.75	0.408	(110)
	29.6	0.302	(104)
HCLV4	22.25	0.399	(110)
	30.1	0.297	(104)
HCLV5	21.95	0.405	(110)
	29.9	0.299	(104)
HCLV6	21.95	0.405	(110)
	29.85	0.299	(104)
HCLL1	22.1	0.402	(110)
	29.95	0.298	(104)
HCLL2	21.75	0.408	(110)
	29.6	0.302	(104)
HCLL3	22.05	0.403	(110)
	29.95	0.298	(104)
HCLL4	22.4	0.397	(110)
	30.3	0.295	(104)
HCLL5	21.8	0.407	(110)
	29.7	0.301	(104)
HCLL6	21.9	0.406	(110)
	29.8	0.299	(104)

Yang et al. [26] discovered that the filler-network structure formed by SiO₂ particles existing around EPDM showed good dispersion in the PP matrix, which improved the mechanical properties and decreased the d-spacing of SiO₂ particles of the composites. Ma et al. [27] reported that POE, as a shell in a PP/POE/CaCO₃ composite, encapsulated CaCO₃ to improve the impact strength in comparison with PP/POE composite and pure PP. The XRD peaks of pure HDPE and HDPE/CaCO₃/LDPE-g-MA/POE composites are shown in Fig. 2. The composites revealed no peak for new crystal planes related to HDPE/CaCO₃/LDPE-g-MA/POE composites.

However, results of the d-spacing of HDPE/CaCO₃/LDPE-g-MA/POE composites by Eq. (1) are shown in Table 2. The d-spacing of HDPE slightly increased in all the composites, while the d-spacing of CaCO₃ slightly decreased. Furthermore, the d-spacing of CaCO₃ on the composites was lower than that of the composite without POE [13]. This may be because of the core-shell structure caused by the POE in the HDPE/CaCO₃/LDPE-g-MA/POE composites, which produced a tensile strength that was higher than the tensile strength reported by Ahn et al. [13]. In addition, it is assumed that maleic anhydride, the polar group of LDPE-g-MA, can improve the surface behavior [28]. This result is consistent with the result obtained in the previous study, which found that the POE particles in the HDPE matrix were coarsened due to the difference in the surface tension, which improved the mechanical properties [29]. The results of described above indicate that the polar groups of the LDPE-g-MA enabled good dispersion of the CaCO₃ particles in the HDPE matrix, and that the core-shell structure of the composites formed by the POE addition resulted in higher tensile strength than that of the composite without POE.

3. TGA Analysis

The TGA curves of HDPE/CaCO₃/LDPE-g-MA/POE composites are indicated in Fig. 3. The thermal stability, such as the temperature at 25% of weight loss ($T_{25\%}$), the temperature at 50% weight loss ($T_{50\%}$), and the temperature at the end of degradation (T_e), is shown in Table 3. The thermal stability of the prepared composites was better than that of HDPE at all temperatures. This may be because the CaCO₃ particles served as a heat barrier [13]. The ther-
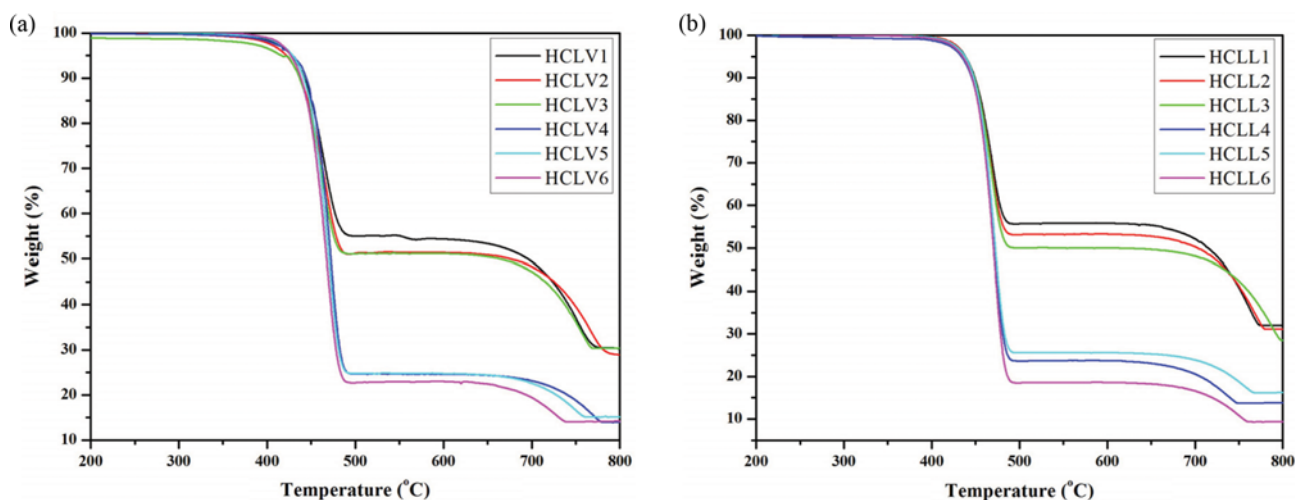
Fig. 3. TGA curves of composites: (a) HDPE/CaCO₃/LDPE-g-MA/VM POE composites, (b) HDPE/CaCO₃/LDPE-g-MA/LC POE composites.

Table 3. Estimation of thermal stability of HDPE/CaCO₃/LDPE-g-MA/POE composites

Sample name	$T_{25\%}$ (°C)	$T_{50\%}$ (°C)	T_e (°C)
HDPE	453.98	465.20	485.29
HCLV1	461.41	695.16	782.00
HCLV2	458.29	675.18	781.28
HCLV3	456.33	618.91	777.86
HCLV4	459.81	472.32	778.77
HCLV5	456.92	470.06	753.29
HCLV6	453.89	467.41	740.92
HCLL1	465.09	714.59	774.74
HCLL2	463.77	702.57	775.59
HCLL3	463.27	532.575	784.27
HCLL4	459.74	471.57	745.72
HCLL5	461.23	472.57	760.62
HCLL6	459.24	470.41	761.26

mal stability was slightly higher in the samples, including more CaCO₃ particles. Overall, the thermal stability of the composites with LC POE was higher than that of the composites with VM POE.

An interesting finding was that the T_e decreased as the ratio of VM POE increased, while the Te increased as the ratio of LC POE increased. The increase in T_e with increasing ratio of LC POE may be because LC POE formed a better core-shell structure with the CaCO₃ particles. This result also supports that the composites with LC POE may provide higher tensile strength in comparison with the composites with VM POE. These results show that the thermal stability of the composites with LC POE was generally higher than that of the composites with VM POE. The T_e was increased as the ratio of LC POE was increased, but improved tensile strength may be obtained by adding a suitable amount of POE.

4. DSC Analysis

The DSC curves of HDPE and the HDPE/CaCO₃/LDPE-g-MA/POE composites at a cooling rate of 5 °C/min are shown in Fig. 4. The crystallization peaks of all the composites were similarly exo-
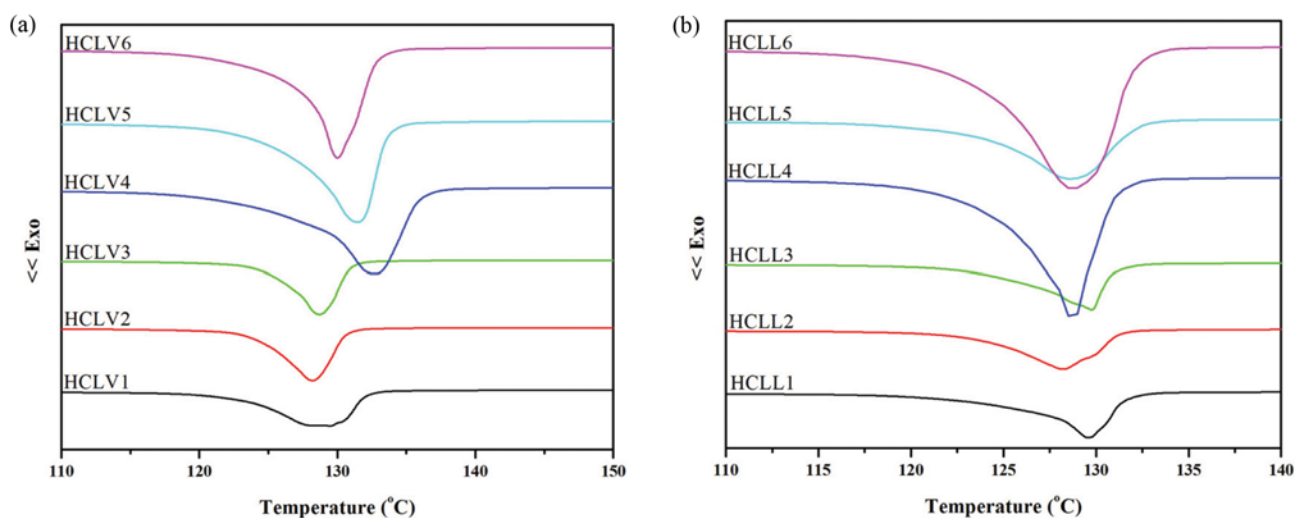

Fig. 4. DSC curves of composites: (a) HDPE/CaCO₃/LDPE-g-MA/VM POE composites, (b) HDPE/CaCO₃/LDPE-g-MA/LC POE composites.

Table 4. The crystallization parameters of HDPE/CaCO₃/LDPE-g-MA/POE composites

Sample name	T_f (°C)	T_c (°C)	T_o (°C)	ΔH_c (J/g)	X_c (%)	ΔS_c (J/g·°C)
HCLV1	126.62	129.61	140.31	42.86	32.92	0.3307
HCLV2	123.42	128.20	139.35	38.71	27.66	0.3019
HCLV3	125.33	129.76	138.58	39.77	27.15	0.3065
HCLV4	126.31	132.05	142.46	106.50	47.71	0.8065
HCLV5	127.08	132.38	141.97	102.50	45.08	0.7743
HCLV6	127.07	132.73	144.21	111.20	48.30	0.8378
HCLL1	122.93	129.52	137.34	41.42	31.81	0.3197
HCLL2	124.25	128.20	136.14	39.81	28.45	0.3105
HCLL3	125.82	128.70	137.79	38.76	26.46	0.3011
HCLL4	127.68	128.94	145.23	108.70	48.69	0.8189
HCLL5	126.55	129.61	147.76	107.60	47.32	0.8185
HCLL6	127.63	128.66	139.67	96.80	42.04	0.7445

thermic. Table 4 shows the crystallization onset temperature (T_o), the crystallization temperature (T_i), the crystallization finishing temperature (T_f), the crystallinity (X_c), and the conformational change (ΔS_c) of the composites.

The T_c of all the composites was higher in the samples contain-

ing more HDPE. The HCLM3 and seven samples having the same weight ratios without POE were compared [13]; the result showed that the crystallization temperature of HDPE/CaCO₃/LDPE-g-MA/POE composites was higher. This may reduce the cycle time in an industrial process, and improve economic feasibility. In addition, the X_c via Eq. (2) of all the composites decreased with increasing the POE content. The X_c of composites has been known to be correlated with ΔS_c. The ΔS_c of the macromolecules was calculated by using Eq. (3). The X_c and ΔS_c were higher in the samples containing more HDPE. The ΔS_c of all the composites was decreased as the ratio of POE was increased. This decrease in ΔS_c may be due to the decrease in the macromolecular space caused by the formation of the core-shell structure of POE and CaCO₃ in the composites. The decreased mobility of the macromolecules of X_c and ΔS_c, similar to the lower d-spacing of CaCO₃ by the core-shell structure in a tendency in XRD peaks, indicates that the CaCO₃ particles were well-dispersed. The results described above show that an appropriate ratio of POE added to the composites may form a core-shell structure, increasing the crystallization temperature, and that the weight ratio of the matrix and the inorganic substances plays a critical role in obtaining improved X_c and ΔS_c.

5. Nonisothermal Crystallization Behavior

The nonisothermal crystallization behavior of the HCLL4 sample that showed the highest tensile strength of the composites was
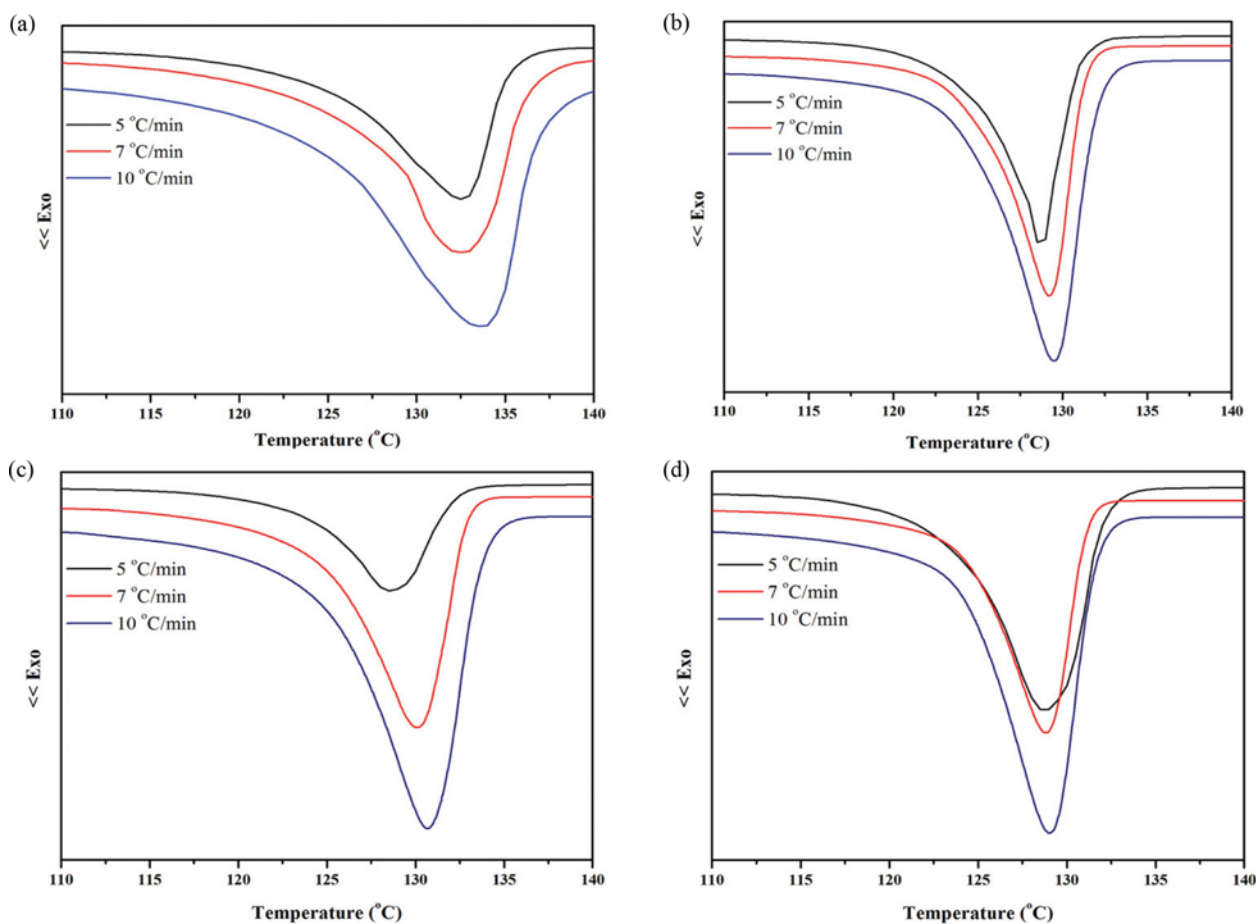

Fig. 5. DSC curves at different cooling rates: (a) HDPE, (b) HCLL4, (c) HCLL5, and (d) HCLL6.

Table 5. The crystallization temperature and half crystallization time at different cooling rates for HDPE, HCLL4, HCLL5, and HCLL6

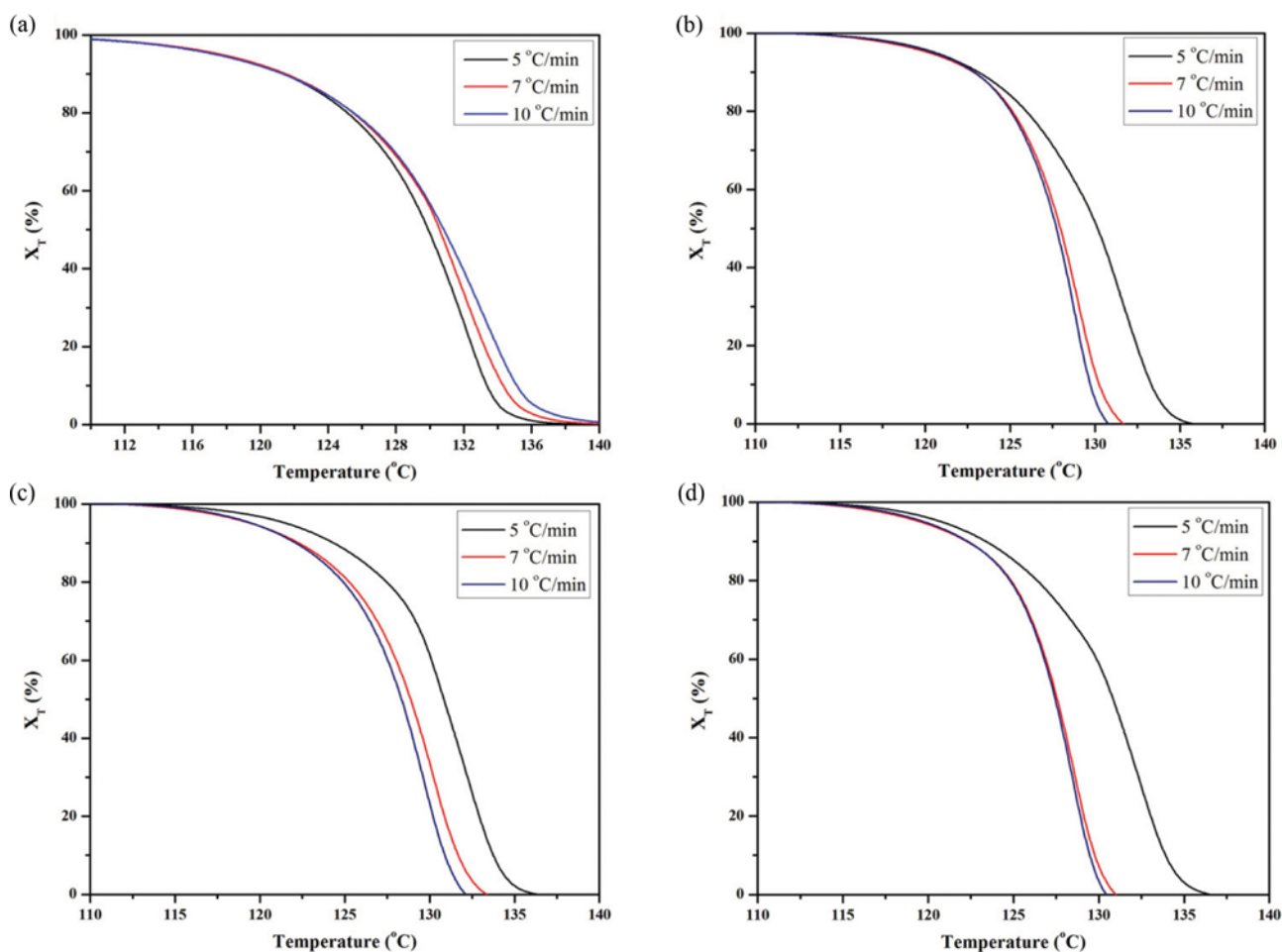| Sample name	α (°C/min)	T_c (°C)	$t_{1/2}$ (min)
HDPE	5	132.45	2.02
	7	133.04	1.35
	10	133.67	0.92
HCLL4	5	128.94	1.13
	7	129.23	0.53
	10	129.50	0.49
HCLL5	5	129.61	1.16
	7	130.12	0.36
	10	130.68	0.33
HCLL6	5	128.66	1.14
	7	128.81	0.33
	10	129.02	0.27

compared with that of the HCLL5, six samples and HDPE. The DSC data obtained at various cooling rates are shown in Fig. 5 and Table 5. The X_T obtained from using Eq. (4) was compared to HDPE and the composites, and the results are shown in Fig. 6.

The composites and HDPE show a sigmoid plot due to a lag effect in the cooling rate during crystallization. In addition, the X-axis of Fig. 6 was converted into crystallization time by using Eq. (5) to draw the plot in Fig. 7. The half crystallization time ($t_{1/2}$), representing the time required for X_t to be 50%, is widely used to present the crystallization rate in Table 5. The average $t_{1/2}$ of the composites was faster than that of HDPE at a given cooling rate, and the $t_{1/2}$ of the HCLL6 sample was the fastest. The results described above indicate that the core-shell structure played the role of stable nucleating agent and thus the crystallization temperature of the composites without POE was higher [13]. The $t_{1/2}$ of composites by core-shell structure was predicted to accelerate the crystallization rate. To verify this prediction in detail, the Avrami model was used to analyze the nonisothermal crystallization kinetics of HDPE and HCLL4, 5, and 6 samples.

6. Non-isothermal Crystallization Kinetic and Activation Energy

The n and Z_t values of the Avrami model were obtained from the slope and intercept of Eq. (6). However, studies have been conducted on the non-isothermal crystallization behavior under conditions that are similar to the actual process. Jeziorny stated that the effect of cooling rate on Z_c should be verified [19]. The effect was investigated as shown in Fig. 8 and Table 6.

The Avrami exponent, n of the composites was smaller than

Fig. 6. Relative crystallinity with various temperature at different cooling rates: (a) HDPE, (b) HCLL4, (c) HCLL5, and (d) HCLL6.
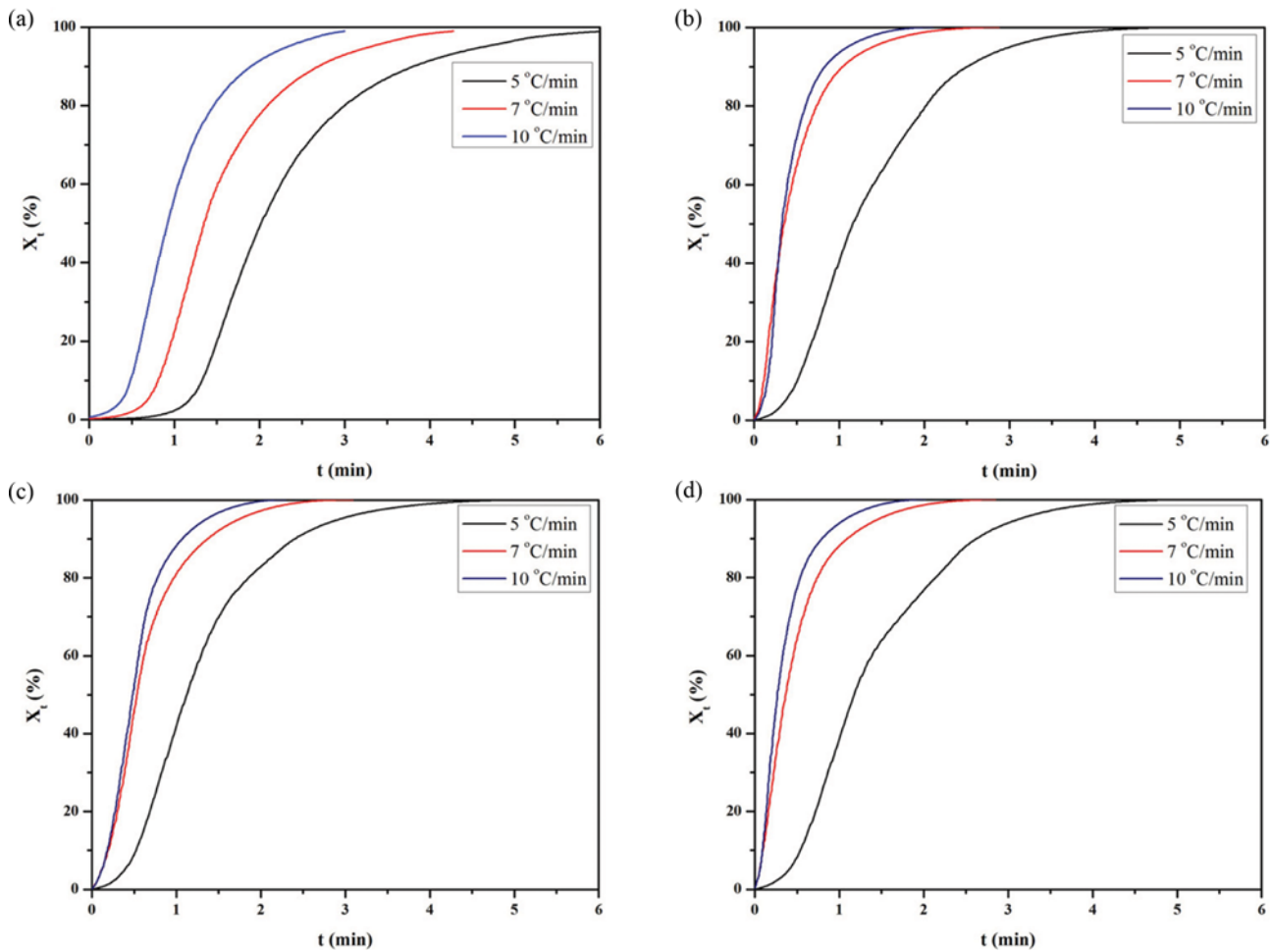
Fig. 7. Relative crystallinity in related to crystallization time at different cooling rates: (a) HDPE, (b) HCLL4, (c) HCLL5, and (d) HCLL6.

Table 6. Non-isothermal crystallization parameters by the Avrami model, Jeziorny's method, and activation energy by the Kissinger method

Sample name	α (°C/min)	n	$\ln Z_t$	Z_c	R^{2a}	E_a (kJ/mol)	R^{2b}
	5	2.43	−2.63	1.69	0.91		
HDPE	7	2.09	−1.38	1.22	0.94	786.21	1
	10	1.77	−0.40	1.04	0.94		
	5	1.8128	−0.833	0.8465	0.985		
HCLL4	7	1.2748	0.392	1.0576	0.990	1671.885	0.99716
	10	1.5700	0.699	1.0724	0.988		
	5	1.8043	−0.862	0.8415	0.994		
HCLL5	7	1.4498	0.722	1.1086	0.987	882.568	0.99983
	10	1.5685	0.997	1.1048	0.977		
	5	1.7977	−0.916	0.8327	0.990		
HCLL6	7	1.2094	0.719	1.1082	0.992	816.160	0.9808
	10	1.2914	1.095	1.1157	0.986		

[a]R^2 of the crystallization kinetic
[b]R^2 of the activation energy

that of HDPE. This result is similar to the report that the irregular distribution of nucleation sites influenced the crystallization rate [30]. In addition, while the Z_c via Eq. (7) values of the three types of composites were lower than that of HDPE, the Z_c value of HCLL6 in which the POE ratio was the highest was the fastest in the composite, indicating a tendency similar to that of the $t_{1/2}$. These
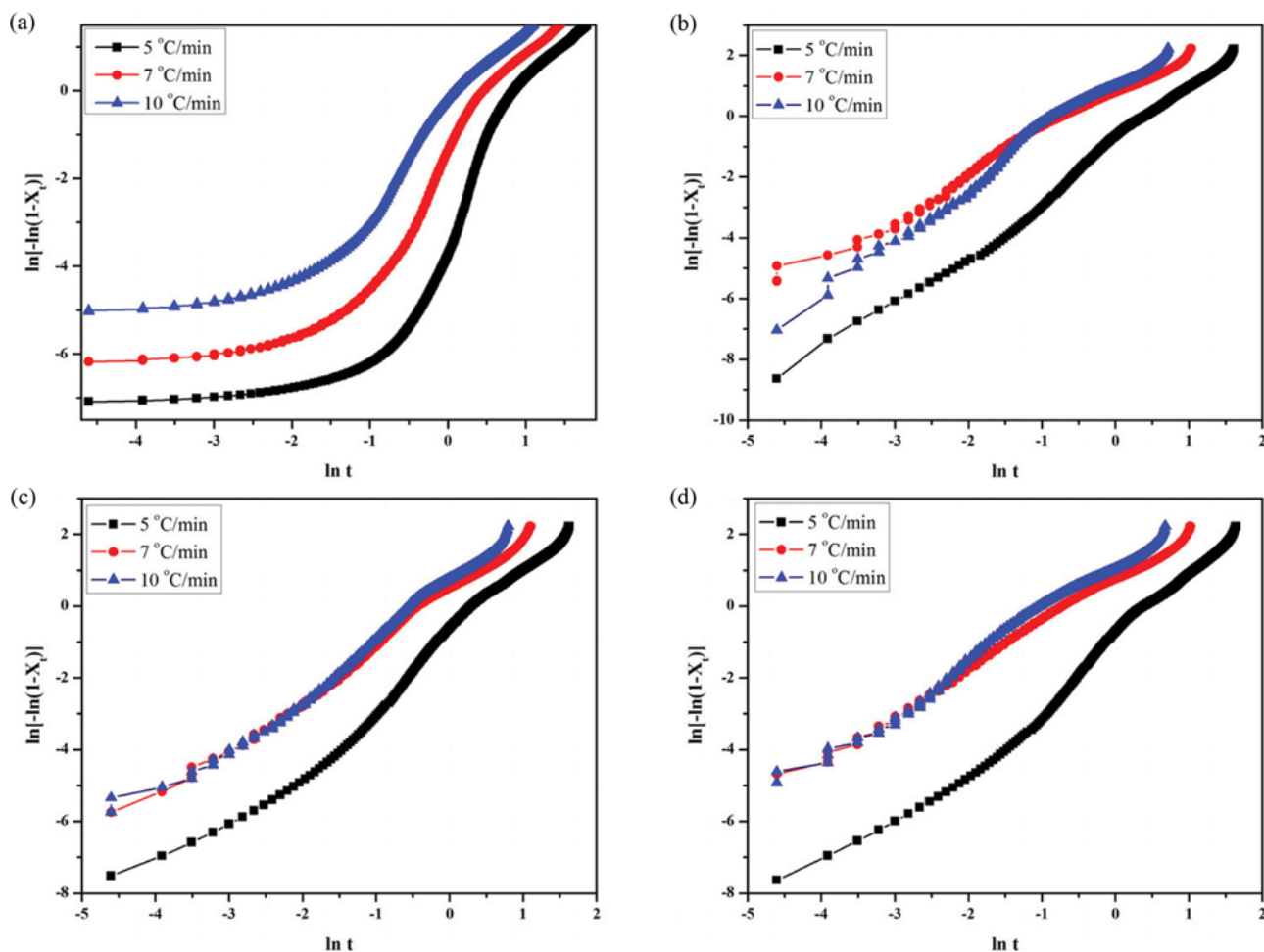
Fig. 8. Non-isothermal crystallization in related to crystallization time at different cooling rates: (a) HDPE, (b) HCLL4, (c) HCLL5, and (d) HCLL6.

results indicate that the n value was decreased by the irregular nucleation distribution due to the core-shell structure of the POE and CaCO₃ particles in the composites, resulting in an acceleration in the Z_c as crystallization rate in the composites expect of HDPE. Furthermore, Table 6 shows the E_a of HDPE and the three composites. The E_a of the composites was higher than that of HDPE, but it decreased as the ratio of added POE was increased in the composites. The E_a result was consistent with the $t_{1/2}$ and Z_c values with increasing POE in the composites. This result indicates that inorganic substances added to composites may show a dispersing effect of CaCO₃ through the core-shell structure of added POE, enabling it to carefully overcome the difficulty of the high E_a [31-33]. The results indicate that LDPE-g-MA helped the dispersion of CaCO₃ particles in the composites. Moreover, the addition of POE formed a core-shell structure, which accelerated the crystallization rate and accomplished efficient E_a.

CONCLUSION

We compared the effects of adding POE on the physical properties of HDPE and HDPE/CaCO₃/LDPE-g-MA/POE composites. The tensile strengths of the composites decreased as the ratio

of POE was increased, and the 28.4 MPa (HCLL4) of the highest tensile strength was shown to be better than 15 MPa (HCLM7) of tensile strength of composites without POE [13] as the same weight ratio of HDPE, CaCO₃, and LDPE-g-MA. Although no novel crystal structure was found in the composites, the addition of POE formed a core-shell structure that reduced the d-spacing of CaCO₃. The thermal stability was better in the composites containing more CaCO₃. With regard to thermal stability, the thermal degradation temperature of the HDPE/CaCO₃/LDPE-g-MA/POE composites was higher than that of HDPE over the entire temperature range. In addition, the X_c and ΔS_c of the composites were reduced as the ratio of POE was increased, indicating that the core-shell structure that formed in the composites enabled well-dispersion of the CaCO₃ particles. The Z_c and E_a of the composites were lower and higher than those of HDPE, respectively. However, the Z_c and E_a of the composites were accelerated and decreased as the ratio of added POE was increased in the composites. The core-shell structure by adding POE in the composites may have acted as a stable nucleating agent to accelerate the Z_c as crystallization rate, enabling efficient E_a to be obtained. The composites prepared in the present study may have potential as materials for the production of electric wire and the lightening of automobiles.

ACKNOWLEDGEMENTS

REFERENCES

1. G. Holden, N. R. Legge and R. P. Quirk, *In Thermoplastic Elastomers: A comprehensive Review*, Hanser, New York (1996).
2. C. C. Honeker and E. L. Thomas, *Chem. Mat.*, **8**, 1702 (1996).
3. K. Petcharoen and A. Sirivat, *Curr. Appl. Phys.*, **13**, 1119 (2013).
4. S. Tunc, O. Duman and T. G. Polat, *Carbonhydr. Polym.*, **150**, 259 (2016).
5. S. Tunc and O. Duman, *Appl. Clay Sci.*, **48**, 414 (2010).
6. S. Tunc and O. Duman, *LWT-Food Sci. Technol.*, **44**, 465 (2011).
7. H. Yang, X. Zhang, C. Qu, B. Li, L. Zhang, Q. Zhang and Q. Fu, *Polymer*, **48**, 860 (2007).
8. M. Valera-Zaragoza, E. Ramírez-Vargas, F. J. Medellín-Rodríguez and B. M. Huerta-Martínez, *Polym. Degrad. Stabil.*, **91**, 1319 (2006).
9. M. Guo, X. Zhou, G. Dai and F. Hu, *Polym. Polym. Compos.*, **13**, 173 (2005).
10. Y. Tsai, J. H. Wu, Y. T. Wu, C. H. Li and T. Leu, *Sci. Technol. Adv. Mater.*, **9**, 1 (2008).
11. F. H. Su and H. X. Huang, *J. Appl. Polym. Sci.*, **112**, 3016 (2009).
12. C. G. Ma, Y. L. Mai, M. Z. Rong, W. H. Ruan and M. Q. Zhang, *Compos. Sci. Technol.*, **67**, 2997 (2007).
13. Y. Ahn, J. H. Jeon, J. H. Park, T. Thenepalli, J. W. Ahn and C. Han, *Korean J. Chem. Eng.*, **33**, 3258 (2016).
14. K. Wang, F. Addiego, N. Bahlouli, S. Ahzi, Y. Rémond and V. Toniazzo, *Compos. Sci. Technol.*, **95**, 89 (2014).
15. M. Alimardani, M. Razzaghi-Kashani and M. H. R. Ghoreishy, *Mater. Des.*, **115**, 348 (2017).
16. B. Wunderlich and M. Dole, *J. Polym. Sci.*, **24**, 201 (1957).
17. R. H. Elleithy, I. Ali, M. A. Ali and S. M. Al-Zahrani, *J. Appl. Polym. Sci.*, **117**, 2413 (2010).
18. M. Avrami, *J. Chem. Phys.*, **7**, 1103 (1939).
19. A. Jeziorny, *Polymer*, **19**, 1142 (1978).
20. H. E. Kissinger, *Anal. Chem.*, **29**, 1702 (1957).
21. J. Z. Liang, B. Zhu and W. Y. Ma, *Polym. Comps.*, **37**, 539 (2016).
22. T. Xie, H. Liu, Y. Ou and G. Yang, *J. Appl. Polym. Sci.*, **101**, 3361 (2006).
23. W. D. M. Sampath, D. G. Edirisingle and S. M. Egodage, DOI:10.1109/MERCon.2015.7112350 (2015).
24. K. C. Seavey, Y. A. Liu and N. P. Khare, *Ind. Eng. Chem. Res.*, **42**, 5354 (2003).
25. P. Svoboda, S. Poongavalappil, R. Theravalappil, D. Svobodova and P. Mokrejs, *Polym. Int.*, **62**, 184 (2013).
26. H. Yang, X. Zhang, C. Qu, B. Li, L. Zhang, O. Zhang and Q. Fu, *Polymer*, **48**, 860 (2007).
27. C. G. Ma, Y. L. Mai, M. Z. Rong, W. H. Ruan and M. Q. Zhang, *Compos. Sci. Technol.*, **67**, 2997 (2007).
28. Y. Long and R. A. Shanks, *J. Appl. Polym. Sci.*, **61**, 1877 (1996).
29. F. M. Mirabella, *J. Polym. Sci. Polym. Phys.*, **32**, 1205 (1994).
30. N. X. Sun, X. D. Liu and K. Lu, *Scr. Mater.*, **34**, 1201 (1996).
31. J. Li, C. Zhou and W. Gang, *Polym. Test.*, **22**, 217 (2003).
32. Y. C. Kim, S. J. Lee, J. C. Kim and H. Cho, *Polym. J.*, **37**, 206 (2005).
33. J. S. Michael, S. A. Abdulwahab, F. S. Kurt, S. Anongnat and V. Priya, *Macromolecules*, **34**, 1864 (2001).